UCRL-JRNL-226993

Uranium-lead isotope systematics of Mars inferred from the basaltic shergottite QUE 94201

A. M. Gaffney, L. E. Borg, J. N. Connelly.

December 27, 2006

Geochimica et Cosmochimica Acta

Uranium-lead isotope systematics of Mars inferred from the basaltic shergottite QUE 94201

Amy M. Gaffney[1]*
Lars E. Borg[1]
James N. Connelly[2]

December 22, 2006

1 – Institute of Meteoritics, University of New Mexico, Albuquerque, NM 87131
now at: Lawrence Livermore National Laboratory, Chemical, Materials and Life Science Directorate, 7000 East Avenue, L-231, Livermore, CA 94550

2 – The Jackson School of Geosciences, 1 University Station C1100, The University of Texas at Austin, Austin, TX 78712
currently at: Geological Institute, University of Copenhagen, Øster Voldgade 10, 1355 København DK

* corresponding author: gaffney1@llnl.gov, 925-422-4396 (ph), 925-422-3160 (fax)

ABSTRACT

Uranium-lead ratios (commonly represented as $^{238}U/^{204}Pb = \mu$) calculated for the sources of martian basalts preserve a record of petrogenetic processes that operated during early planetary differentiation and formation of martian geochemical reservoirs. To better define the range of μ values represented by the source regions of martian basalts, we completed U-Pb elemental and isotopic analyses on whole rock, mineral and leachate fractions from the martian meteorite Queen Alexandra Range 94201 (QUE 94201). The whole rock and silicate mineral fractions have unradiogenic Pb isotopic compositions that define a narrow range ($^{206}Pb/^{204}Pb = 11.16 – 11.61$). In contrast, the Pb isotopic compositions of weak HCl leachates are more variable and radiogenic. The intersection of the QUE 94201 data array with terrestrial Pb in $^{206}Pb/^{204}Pb$ – $^{207}Pb/^{204}Pb$ – $^{208}Pb/^{204}Pb$ compositional space is consistent with varying amounts of terrestrial contamination in these fractions. We calculate that only 1-7% contamination is present in the purified silicate mineral and whole rock fractions, whereas the HCl leachates contain up to 86% terrestrial contamination. Despite the contamination, we are able to use the U-Pb data to determine the initial $^{206}Pb/^{204}Pb$ of QUE 94201 (11.086 ± 0.008) and calculate the μ value of the QUE 94201 mantle source to be 1.823 ± 0.008. This is the lowest μ value calculated for any martian basalt source, and, when compared to the highest values determined for martian basalt sources, indicates that μ values in martian source reservoirs vary by at least 100%. The range of source μ values further indicates that the μ value of bulk silicate Mars is approximately three. The amount of variation in the μ values of the

mantle sources ($\mu \sim 2$-4) is greater than can be explained by igneous processes involving silicate phases alone. We suggest the possibility that a small amount of sulfide crystallization may generate large extents of U-Pb fractionation during formation of the mantle sources of martian basalts.

1. INTRODUCTION

The U-Pb elemental and isotopic systematics of the planets are controlled by a variety of poorly characterized factors including their bulk composition and volatile element budgets, metal-silicate partitioning of Pb during core formation, and U-Pb fractionation associated with silicate differentiation. These phenomena are difficult to quantify because U-Pb isotope systematics of samples from differentiated bodies are often disturbed by impact metamorphism and alteration at the planet's surface. In addition, partitioning of Pb in silicate and metal-silicate systems can be strongly controlled by trace phases, such as sulfides, the presence or absence of which is not constrained by experimental studies of phase equilibria. Despite these difficulties, several general observations about the U-Pb isotope systematics of differentiated bodies can be made. First, silicate differentiation involving olivine, pyroxene, plagioclase, spinel and/or garnet does not significantly fractionate U from Pb. On Earth, this is manifest in the limited variation of the $^{238}U/^{204}Pb$ ratios (μ values) inferred for source reservoirs from the Pb isotopic compositions of modern basalts and chemically differentiated crustal rocks. Second, terrestrial, lunar, and martian basalt source regions are characterized by vastly different μ values (e.g., Chen and Wasserburg; Premo et al., 1999; Borg et al., 2005). This implies that there are fundamental differences in the bulk compositions of these bodies and/or the mechanisms by which U and Pb are fractionated during planetary evolution. Finally, very few if any rocks from differentiated bodies show evidence for undisturbed U-Pb isotope

systematics. In order to better understand the behavior of U and Pb on Mars, as well as to better understand mechanisms that contribute to differences in the U-Pb systematics of different planets, we have completed U-Pb isotopic analyses of the martian meteorite Queen Alexandra Range 94201 (hereafter 'QUE').

The meteorite QUE is derived from a source region that is characterized by very low abundances of the most incompatible elements. In fact, QUE represents the end-member in the compositional continuum of martian meteorites. It has the lowest initial $^{87}Sr/^{86}Sr$ ratio, the highest initial ε_{Nd} value (Borg et al., 1997), and the most light rare earth element (LREE)-depleted REE pattern (e.g., Lodders, 1998) of all martian meteorites. The other end of the continuum is defined by meteorites such as Zagami. In contrast to QUE, Zagami has the highest initial $^{87}Sr/^{86}Sr$ ratios, lowest initial ε_{Nd} value (Borg et al., 2005), and one of the most LREE-enriched REE patterns. The enormous range of incompatible trace element abundances and Sr and Nd isotopic compositions observed in the martian meteorite suite has been attributed to extreme elemental fractionation in their source regions as a result of solidification of a martian magma ocean (e.g., Borg et al., 1997; Blichert-Toft et al., 1999; Brandon et al., 2000; Borg and Draper, 2003; Borg et al., 2003). In this hypothesis, the meteorites with trace element and isotopic signatures indicative of derivation from the most depleted source regions represent differentiates of melts of early-formed magma-ocean cumulates consisting primarily of olivine and pyroxene. The meteorites with elemental and isotopic signatures indicative of formation from the most evolved sources are derived from reservoirs comprising late-stage crystallization products of the martian magma ocean. By comparing the results of this

study on QUE to results from previous studies on meteorites from more evolved source regions, we will be able to assess whether early differentiation on Mars fractionated U from Pb. Furthermore, these results will define the magnitude of Pb isotopic variations in the martian mantle, determine if correlations between the Pb and Sr, Nd and Hf isotopic compositions in the martian mantle exist, and provide constraints on mechanisms by which U can be fractionated from Pb in the martian interior.

Only a few U-Pb isotopic studies have been completed on martian samples. This stems from the fact that many of the samples contain both martian and terrestrial contamination (Borg et al., 2005) and are characterized by low concentrations of incompatible trace elements, including Pb. As a consequence, the majority of detailed Pb isotopic studies have focused on the most evolved, Pb-enriched samples. Nevertheless, all U-Pb isotope data sets from martian meteorites demonstrate evidence for isotopic disturbance. Thus, the only way to determine the Pb isotopic compositions of the source regions is to evaluate the U-Pb isotope systematics of the meteorites in the context of their crystallization ages determined with other age dating techniques. The crystallization age of QUE is well-defined to be 327 ± 10 Ma (weighted average of Rb-Sr and Sm-Nd ages determined by Borg et al., 1997) and belongs to a growing group of ~330 Ma martian basalts that includes NWA 1195 (Symes et al., 2005) and NWA 1460 (Nyquist et al., 2004). Thus, even the partially disturbed U-Pb isotope systematics of QUE will provide constraints on the U-Pb isotopic evolution of the QUE source region.

2. ANALYTICAL PROCEDURES

2.1. Preparation of mineral fractions

Initial mineral separation and leaching steps were carried out at the University of New Mexico. These procedures are shown schematically in Fig. 1. A piece of QUE weighing 325 mg was allocated to us by the Meteorite Working Group at Johnson Space Center. A chip weighing 33 mg was crushed to fine powder with a sapphire mortar and pestle for the whole rock analysis. The remaining sample was crushed and sieved to various grain size fractions. The 100-200 mesh (75-150 μm) grain size fraction was further processed using a Frantz isodynamic magnetic separator to make oxide-rich, Fe-pyroxene-rich, Mg-pyroxene-rich and plagioclase-rich fractions. These fractions were purified by hand-picking in ethanol to visually-estimated purity levels of > 99.5%. The parts of the mineral fractions rejected during hand-picking are designated with the suffix 'rej'. The reject fractions consist of composite and single-mineral grains and impact-melt glass.

Purified mineral separates and mineral reject fractions were washed in 0.5 N acetic acid in an ultrasonic bath for 10 minutes at room temperature, followed by a wash with quartz-distilled water. The mineral fractions were then leached in HCl, in an ultrasonic bath, for 10 minutes at room temperature. The oxide fractions were leached in 1 N HCl and the silicate fractions were leached in 2 N HCl. The leached residues are designated with the suffix '(R)' and the HCl leachates are designated with the suffix '(L)'. After leaching, the

mineral fractions were washed in quartz-distilled water and this final water rinse was combined with the HCl leachate of each fraction for U and Pb isotopic analysis.

During hand-picking, individual phosphate grains and composite grains containing phosphate were identified and separated. These grains were washed with acetic acid and the phosphates were preferentially dissolved with 2 N HCl. Residues from this step, which were mostly interstitial silicate grains, were not processed further.

2.2. Chemical separations and mass spectrometry

Sample digestion, column chemistry and mass spectrometry were completed at The University of Texas at Austin. The mineral fractions were dissolved with $HF+HNO_3+HCl$ and spiked with a mixed ^{235}U-^{205}Pb tracer. Lead was purified on anion resin columns using HBr and HCl (Borg et al., 2005). Uranium was purified with UTEVA U-specific resin and HNO_3. Samples were run on a Finnigan MAT 261 thermal ionization mass spectrometer, in static mode using an all Faraday cup acquisition routine. Procedural blanks for dissolution + column chemistry were measured to be less than 2.5 pg Pb, and sample-blank ratios range from 135 to 3260 for the mineral fractions. Total uncertainties on the Pb isotopic compositions reported in Table 1 reflect the combination of uncertainties determined for the internal analytical precision as well as corrections for mass fractionation and laboratory blank, and are typically less than 0.1% for $^{206}Pb/^{204}Pb$ and $^{207}Pb/^{204}Pb$, and less than 0.05% for $^{207}Pb/^{206}Pb$.

3. U-PB ISOTOPE DATA

3.1. Results

3.1.1. Lead isotope results

Lead isotopic compositions in the silicate mineral fractions (pure and reject) define a narrow range characterized by unradiogenic isotope ratios. In these fractions, $^{206}Pb/^{204}Pb$ ranges from 11.16 to 11.61, $^{207}Pb/^{204}Pb$ ranges from 11.47 to 11.72 and $^{208}Pb/^{204}Pb$ ranges from 31.14 to 31.56. Lead in the oxide fractions (pure and reject) is more radiogenic than in the silicate fractions, whereas the phosphate fraction is the most radiogenic of all the mineral fractions ($^{206}Pb/^{204}Pb$ = 15.12, $^{207}Pb/^{204}Pb$ = 13.61 and $^{208}Pb/^{204}Pb$ = 34.75). The isotopic composition of Pb in the HCl leachates is highly variable, with some leachates approaching the composition of modern terrestrial Pb. On a conventional $^{206}Pb/^{204}Pb$ – $^{207}Pb/^{204}Pb$ diagram, all the fractions (pure minerals, rejects, whole rock and leachates) define a linear array, the slope of which corresponds to an age of 4325 ± 21 Ma (MSWD = 66; Fig. 2a). A line regressed through only the mineral (pure and reject) and whole rock fractions is indistinguishable from the line defined by all fractions and corresponds to an age of 4342 ± 23 Ma (MSWD = 32). The pure silicate mineral fractions (Plag (R), Fe-Px (R), Mg-Px (R)), which are the fractions most likely to be free of impact melt glass, define only a poor approximation of a line, as illustrated by the large uncertainty on the age, 3944 ± 2000 Ma, derived from the slope of this array.

The mineral fractions and leachates also define a poorly-correlated linear array in $^{206}Pb/^{204}Pb$ – $^{208}Pb/^{204}Pb$ compositional space (Fig. 2b). In detail, the array defined by all fractions (pure minerals, reject minerals, whole rock and leachates) is offset to slightly higher $^{208}Pb/^{204}Pb$ and has a slightly steeper slope than the array defined by the silicate fractions alone. This reflects the leverage of the Ox (R), Ox-rej (R) and WR (L) fractions on the geometry of the array. These fractions have slightly higher $^{208}Pb/^{204}Pb$ at a given $^{206}Pb/^{204}Pb$ than the silicate mineral and leachate fractions, and therefore lie slightly above the line regressed through the silicate mineral and silicate leachate fractions.

3.1.2. Uranium-lead results

The QUE fractions show considerable scatter on both the $^{238}U/^{204}Pb$-$^{206}Pb/^{204}Pb$ and $^{235}U/^{204}Pb$-$^{207}Pb/^{204}Pb$ diagrams (Fig. 3). In the silicate mineral and whole rock fractions, the μ value varies from 1.22 to 4.32, a range consistent with a relatively minor amount of U-Pb fractionation among the respective mineral phases during igneous crystallization. In both U-Pb diagrams, the silicate fractions (pure minerals, rejects and whole rock) cluster in shallow, poorly-defined arrays. The oxide fractions have low μ values similar to those of the silicate fractions, which contrast with the relatively radiogenic $^{206}Pb/^{204}Pb$ compositions of these fractions. The phosphate fraction has the highest μ value of all mineral fractions: 6.17. The μ values of leachates are slightly higher than those of the silicate fractions, and range from 2.72 to 7.30. This presumably reflects the contribution of phosphate to the leachates. In the ^{238}U-^{206}Pb system, the line with a slope corresponding to the age closest to the crystallization age of 327 Ma (Borg et al., 1997) is

defined by the WR (R), Plag (R) and Mg-Px (R) fractions. The age derived from this line is 397 ± 21 Ma (MSWD = 0.45) and the corresponding initial $^{206}Pb/^{204}Pb$ is 11.086 ± 0.008. As expected, the ^{235}U-^{207}Pb isochron does not record any corresponding age information, given the minimal variability in $^{235}U/^{204}Pb$ among the mineral fractions and the very small amount of ^{207}Pb that was produced by radioactive decay in the last ~330 million years.

3.2. Interpretation of U-Pb data

3.2.1. Lead isotope systematics

Linear variations on a $^{206}Pb/^{204}Pb$ vs. $^{207}Pb/^{204}Pb$ plot can reflect either radiogenic ingrowth such that the array has chronometric significance, or variable mixtures of two components, in which case the array has no chronometric significance. The array defined by the QUE fractions is likely to reflect various mixtures of martian Pb and modern terrestrial Pb because: 1) all fractions analyzed in this study define a single linear array, the extension of which passes through the isotopic composition of modern terrestrial Pb (including Pb in Antarctic ice, Fig. 2a), 2) leachates, which sample the most mobile Pb in the system and therefore are the most likely to contain the largest proportion of terrestrial contamination, plot closest to modern terrestrial Pb, 3) pure mineral residues are typically less radiogenic than their reject counterparts, consistent with the higher proportions of impact melt glass (which is more susceptible to Pb exchange) in the reject fractions, 4) the WR (R) fraction, which should lie within the range of the mineral fractions in a

closed, uncontaminated system, is the least radiogenic fraction, suggesting that contamination was more effectively removed from this finer-grained fraction than from any of the pure mineral fractions, and 5) the ancient age (~4.3 Ga) derived from this array is highly discordant with the independently defined and accepted age of 327 Ma (Borg et al., 1997).

Linear variation on a $^{206}Pb/^{204}Pb$ vs. $^{208}Pb/^{204}Pb$ plot may also reflect either mixing between two components or radiogenic ingrowth. For reasons similar to those outlined above for the $^{206}Pb/^{204}Pb$ - $^{207}Pb/^{204}Pb$ system, the array shown in Fig. 2b also is interpreted to result from mixing between martian Pb and modern terrestrial Pb. Co-linearity of all the mineral fractions resulting from radiogenic ingrowth requires that all the minerals have the same Th/U ratio. However, partition coefficients for U and Th in the mantle assemblage are sufficiently different that is it unlikely that any individual phase will inherit the bulk rock Th/U during crystallization. Thorium concentrations were not determined in this study, so the Th/U ratios of the QUE fractions are not independently known. Terrestrial Pb also falls on the $^{206}Pb/^{204}Pb$ vs. $^{208}Pb/^{204}Pb$ array defined by the QUE fractions. If this array represented radiogenic ingrowth instead of mixing between martian and terrestrial Pb components, it would require the Th/U ratios of QUE and all its fractions to be identical to that of Earth. However, to the best estimate, Mars and Earth have different bulk Th/U (Mars: 3.5, Dreibus and Wänke, 1985; Earth: 3.8, Lodders and Fegley, 1997; Elliot et al., 1999; Zartman and Richardson, 2005), so modern terrestrial Pb should not fall on a $^{206}Pb/^{204}Pb$ vs. $^{208}Pb/^{204}Pb$ array defined by martian Pb. Thus, the most reasonable explanation for this array is that the Pb isotopic

compositions of these mineral fractions represents a mixture between martian and terrestrial Pb.

3.2.2. Uranium-lead systematics

Linearity of data on either the $^{238}U/^{204}Pb$ vs. $^{206}Pb/^{204}Pb$ or the $^{235}U/^{204}Pb$ vs. $^{207}Pb/^{204}Pb$ plot typically indicates that radiogenic Pb evolved in a closed system and that individual phases were initially in Pb isotopic equilibrium but had different μ values. The non-linearity of the QUE data in both U-Pb systems is consistent with terrestrial Pb contamination that generated significant increases in the Pb isotope ratios coupled with moderate decreases in U/Pb ratios. The elevated μ values of some of the leachates (Ox(L), Plag(L)) may also reflect an additional component derived from preferential dissolution of fine-grained, high-μ phosphates from the mineral fractions during exposure to 1N or 2N HCl. Phosphates are abundant in QUE (2.4-5%, Harvey et al., 1996; Mikouchi et al., 1996), dissolve easily in weak (< 2 N) HCl, and have Pb isotopic compositions that are expected to be similar to those of the leachates. Additionally, a high μ value was determined for the phosphate fraction.

The 397 ± 21 Ma age defined by the WR (R), Plag (R) and Mg-Px (R) fractions is not considered a robust age but rather an alignment of slightly disturbed fractions that would define a line with a slope corresponding to an age of ~330 Ma if the fractions were not contaminated by terrestrial Pb. The limited spread in U/Pb makes the age particularly susceptible to disturbance by minor amounts of contamination. Given the slight

disturbance recorded by these three fractions, we conclude that the initial $^{206}Pb/^{204}Pb$ of 11.086 ± 0.008 is a reasonable value for the initial Pb composition of this sample (a more complete discussion on the initial Pb isotopic composition is given in section 4.1). Hence, this ratio represents the Pb isotopic composition of the QUE source region at the time that the source melted to produce the QUE parent magma. The reject silicate mineral fractions fall only slightly above the line defined by the WR (R), Plag (R) and Mg-Px (R) fractions, indicating that they contain only slightly more contamination than the purified mineral fractions. The principal impurity in the reject mineral fractions is impact melt glass, which may render these fractions more susceptible to terrestrial contamination, because the glass may react more efficiently with terrestrial surface contaminants than the minerals do.

3.3. Modeling of terrestrial contamination

The amount of terrestrial contamination can be approximated by two methods (Table 2). Both methods assume the 327 Ma as the age of QUE, and 11.086 as its initial $^{206}Pb/^{204}Pb$. The first method (Pb-Pb method) ignores the minor radiogenic ingrowth of Pb since 327 Ma, thus allowing for the assumption that the measured $^{206}Pb/^{204}Pb$ ratio for a fraction represents a mixture of the initial $^{206}Pb/^{204}Pb$ for the sample (11.086) and the $^{206}Pb/^{204}Pb$ of Antarctic ice (18.79). This method returns estimates of Pb contamination in the mineral fractions that range from 0.015 ng Pb (Plag (R)) to 3.383 ng (Oxide rej) and a total amount of Pb contamination in the processed piece of QUE of 6.074 ng (24% of the total Pb analyzed). This method also estimates ratios of sample Pb to contamination Pb that

range from 0.169 (Plag (L)) to 70.649 (WR (R)) and a ratio for the total sample to contaminant Pb of 3.214.

A second method (U-Pb method) estimates the amount of Antarctic Pb contamination that must be stripped from each fraction to restore a 327 Ma $^{238}U/^{204}Pb$ vs. $^{206}Pb/^{204}Pb$ isochron line with an initial $^{206}Pb/^{204}Pb$ ratio of 11.086. This method returns estimates of Pb contamination in the silicate fractions that range from 0.003 ng (Mg-Px (R), Plag (R)) to 3.291 ng (Ox-rej). Ratios of sample to contaminant Pb range from 0.241 (Plag (L)) to 303.920 (WR (R)).

The amounts of terrestrial contamination estimated with the two methods agree reasonably well. For most fractions, the ratio of the amounts of contamination determined by the two methods is close to unity (Table 2). The fractions with the highest ratios (contamination determined with Pb-Pb method/contamination determined with U-Pb method) and the greatest deviations from unity are also the fractions inferred to be the purest, based on the fact that they give the best approximation of a crystallization age in the ^{238}U-^{206}Pb diagram (Fig. 3a). The large ratios for these three fractions suggest that the Pb-Pb method overestimates Pb contamination in these fractions. The good agreement of the two methods in calculating contamination in the rest of the fractions would not be apparent if the Pb-Pb array primarily reflected radiogenic ingrowth and the scatter on the U-Pb diagram reflected U-Pb fractionation during sample treatment. The consistency between estimates of Pb contamination by the two methods supports our interpretation that all Pb analyses contain varying, and in some fractions significant, amounts of

terrestrial Pb, and that the Pb-Pb array is therefore not chronometrically significant. As expected, the three fractions that define a ^{238}U-^{206}Pb age of 397 Ma (WR (R), Plag (R) and Mg-Px (R)) have the highest sample/contaminant ratios. However, the positive correlation between μ value and sample/contaminant ratio for these three fractions is also consistent with a calculated age that is older than the accepted age.

4. URANIUM-LEAD SYSTEMATICS OF THE MARTIAN MANTLE

Lead behaves as both a lithophile and chalcophile element. It is also highly volatile. Thus, in addition to recording information about silicate differentiation within the planet, the U-Pb systematics of martian meteorites potentially record information about aspects of petrogenesis, such as core formation, the role of sulfides during planetary differentiation, and mobilization of volatile elements, that are not preserved in the lithophile element isotope systematics of Rb-Sr, Sm-Nd or Lu-Hf. In the following sections, we estimate the μ value of the mantle source of QUE and compare this to estimates of the μ values of mantle sources of other martian basalts. By examining variation among μ values of mantle sources in relation to $^{87}Rb/^{86}Sr$, $^{147}Sm/^{144}Nd$ and $^{176}Lu/^{177}Hf$ variation in the mantle sources, we evaluate magma ocean processes that may have generated compositional end-members in the martian mantle.

4.1. Mu values of the shergottite sources

We calculate the long-term μ value of the QUE source using estimates of the initial $^{206}Pb/^{204}Pb$ of QUE and assuming single-stage Pb growth in the QUE source reservoir from 4.558 to 0.327 Ga, starting with Canyon Diablo Troilite (CDT) as the initial Pb isotopic composition. The initial $^{206}Pb/^{204}Pb$ is the only variable we explore, given the lack of information preserved in the ^{235}U-^{207}Pb systematics. As shown in the previous section, Pb isotopic compositions of QUE fractions are affected by differing amounts of terrestrial contamination. In the effort to make the best estimate of the initial $^{206}Pb/^{204}Pb$ of QUE, we employ three different methods of calculation. Each method uses a different set of assumptions, and together they return a maximum range of reasonable estimates. In the first method, which was described in section 3.2.2, the initial $^{206}Pb/^{204}Pb$ is determined to be 11.086 ± 0.008 from the ^{238}U-^{206}Pb isochron, yielding a μ value for the QUE source of 1.82 ± 0.01. The uncertainty on this estimate incorporates only the error on the initial $^{206}Pb/^{204}Pb$, and not the additional uncertainty resulting from the difference between the age determined from this isochron and the accepted age. The second method assumes that the WR (R) fraction, corrected for 327 Ma of radiogenic ingrowth using the measured $^{238}U/^{204}Pb$, represents the initial $^{206}Pb/^{204}Pb$ of QUE. This is based on the observation that the WR (R) is the least radiogenic fraction and thus is likely to be the least contaminated fraction. The corresponding μ value for the source is 1.84 ± 0.01. Because there is probably a small amount of contamination still present in this fraction, this estimate represents a maximum value. The third estimate is made by assuming that the initial Pb isotopic composition of QUE is coincident with the intersection of the array defined by

all QUE fractions and the 327 Ma Geochron. This method assumes single-stage Pb evolution starting with an initial Pb isotopic composition of CDT at 4.558 Ga to define the Geochron, and that deviation of the mineral fractions from the 327 Ma Geochron is due to terrestrial contamination only. As such, this method represents a minimum estimate of the μ value. This calculation yields an initial $^{206}Pb/^{204}Pb$ of $11.02^{+0.02}_{-0.03}$, based on uncertainty on the crystallization age, and a source with $\mu = 1.76^{+0.02}_{-0.03}$. The μ values calculated by the three techniques differ by less than 5%, indicating that terrestrial Pb contamination, errors in the assumptions, and other disturbance to the sample do not have a significant effect on the calculated μ value of the QUE source. The best estimate for the μ value of the QUE source is that determined by the first method, 1.823 ± 0.008, as it utilizes the common method for estimating initial isotopic compositions (i.e., an isochron), and it falls between the values independently determined to be the maximum and minimum values (using methods two and three, respectively). Regardless of the method used, the μ value of the QUE source is the lowest estimated for any shergottite.

The proximity of the first two initial Pb estimates to the 327 Ma Geochron is consistent with an early age for silicate differentiation on Mars, as implied by ^{146}Sm-^{142}Nd and ^{182}Hf-^{182}W studies of martian meteorites (Harper et al., 1995; Borg et al., 1997; Borg et al., 2003; Kleine et al., 2004; Foley et al., 2005). Thus, the Pb data essentially confirm that the QUE source reservoir formed very early in the history of Mars and that it underwent little-to-no chemical modification between the time that it formed and subsequently melted to give rise to the QUE parent magma.

In addition to QUE, the only shergottites for which U-Pb isotopic compositions have been measured on purified, leached mineral fractions are Shergotty, Zagami and Yamato 793605 (Chen and Wasserburg, 1986a; Misawa et al., 1997; Borg et al., 2005). Lead isotope data for LEW 88516, ALH 77005, EETA 79001, Los Angeles and Dar al Gani 476 exist only for leached whole rocks (Chen and Wasserburg, 1986a,1986b, 1993; Bouvier et al., 2005), and of these, U concentrations have been measured for all samples except Dar al Gani 476. The ^{238}U-^{206}Pb isochron for Zagami yields a crystallization age that is concordant with the Rb-Sr and Sm-Nd ages. Thus, the initial $^{206}Pb/^{204}Pb$ determined from the ^{238}U-^{206}Pb isochron and the corresponding estimate for the μ value of the Zagami source (3.96 ± 0.02, Borg et al., 2005) are argued to be reliable. In contrast, U-Pb isotope data for mineral separates of both Shergotty and Yamato 793605 do not define isochrons that are concordant with Rb-Sr and Sm-Nd ages and do not yield robust estimates of the initial $^{206}Pb/^{204}Pb$ of these meteorites. Therefore, for each of these samples, the initial $^{206}Pb/^{204}Pb$ is calculated by correcting the $^{206}Pb/^{204}Pb$ measured on the whole rock fraction for radiogenic ingrowth since the time of crystallization using the measured μ value. For the respective initial Pb isotopic compositions, the estimated source μ values are 4.94 ± 0.02 for Shergotty and 5.12 ± 0.03 for Yamato 793605. Mu values estimated for other shergottite sources (LEW 88516, ALH 77005, EETA 79001, Los Angeles), using this same approach, range from 3.65 to 5.99. However, because only whole rocks (and not mineral fractions) were analyzed for these samples, it is not possible to rigorously evaluate the extent of Pb disturbance in these samples and thus determine if these values truly represent the μ values of the source regions. Therefore, these source μ values should be taken as estimates. Nevertheless, these comparisons

clearly demonstrate that QUE is derived from a source region with a μ value that is significantly lower than those of other martian basalts.

4.2. The bulk μ value of Mars

Previous Pb isotopic studies of individual martian samples have estimated the μ value of the shergottite mantle source region to be ~4-5 (Chen and Wasserburg, 1986a; Borg et al., 2005; Bouvier et al., 2005). This has been inferred to represent the μ value for bulk silicate Mars. However, the new results for QUE require that at least a part of the martian mantle has a μ value of ~1.8. Thus, the μ value of bulk silicate Mars is likely lower than previously inferred. The best estimate is simply the median value determined for the shergottites: ~3. A more precise value will require a rigorous estimation of the size of the low-μ depleted reservoir relative to the higher-μ enriched reservoir, which is sampled in the greater proportion of the shergottites. A bulk silicate martian μ value of 3 is considerably lower than the μ values estimated for both the Moon (~8-35, Premo et al., 1999) and bulk silicate Earth (8-10). These differences may reflect either variable extents of Pb sequestered into the cores of the three bodies, and/or may reflect different abundances of volatile elements in the bulk planets. However, because the Moon is thought to have only a very small core, if any at all, the bulk μ value of the Moon is likely controlled predominantly by the volatility of Pb. This is consistent with the Moon's overall depletion in volatile elements (Taylor, 1980). Conversely, Mars is known to be rich in volatile elements (Dreibus and Wänke, 1985). The broad inverse correlation between bulk μ and bulk $^{87}Rb/^{86}Sr$ of the Moon, Earth and Mars suggests that these

parameters are controlled by the high volatility of Rb and Pb. Thus, core formation appears to play a secondary role in determining the bulk silicate μ value of these three terrestrial bodies.

4.3. Formation of the end-member sources of martian basalts

Mu values calculated for the shergottite sources show broad correlations with $^{87}Rb/^{86}Sr$ and $^{147}Sm/^{144}Nd$ ratios determined for these same sources using initial Sm and Nd isotopic compositions and assuming differentiation at ~4.5 Ga (Fig. 4). This probably reflects mixing between end-member source components during formation of the shergottite magmas. Scatter in these trends is likely to reflect inaccurate estimations of μ values of the sources, resulting from calculations based on whole rock data. However, the source compositions of QUE and Zagami, for which μ values are confidently determined, can be used to constrain the μ values of martian source end-members. The $^{87}Rb/^{86}Sr$, $^{147}Sm/^{144}Nd$ and $^{176}Lu/^{177}Hf$ compositions of QUE and Zagami sources indicate that they sample, respectively, the most incompatible element-depleted and -enriched source components yet identified in the suite of shergottites. Correspondingly, the μ value of the QUE source is the lowest and the μ value of the Zagami source is close to the highest estimated for the shergottites. Regardless of uncertainty in the μ values of the sources of the other shergottites, the compositions of Zagami and QUE require that the enriched end-member has μ of ~4 or greater and that the depleted mantle end-member has μ of ~2 or less. Additionally, the correlation of μ with other parent-daughter ratios suggests that the range

in μ values results from the same geologic processes that generate variation among Rb/Sr, Sm/Nd and Lu/Hf during formation of the martian source reservoirs.

Borg et al. (2003) described variations among $^{87}Rb/^{86}Sr$, $^{147}Sm/^{144}Nd$ and $^{176}Lu/^{177}Hf$ values calculated for shergottite source regions from which they inferred that only two compositional end-members are required in the sources of these samples. One end-member is incompatible element-depleted and the other end-member is incompatible element-enriched. Based on the similarity of these variations in the sources of martian basalts and lunar mare basalts, Borg et al. (2003) inferred that the depleted and enriched martian basalt source end-members are analogous to the compositional end-members in the lunar mantle. The lunar mantle end-members are inferred to have formed from crystallization of the lunar magma ocean (e.g., Snyder et al., 1992), and thus Borg et al. (2003) proposed that the martian source end-members also formed through crystallization of a magma ocean. In models of the lunar magma ocean, mafic cumulates form a depleted mantle end-member, and late-stage trapped liquid components form an enriched mantle end-member (Snyder et al., 1992). Subsequently, Borg and Draper (2003) presented a petrologic and geochemical model for the formation of these two end-members by crystallization of silicates in a martian magma ocean. This relatively simple model successfully reproduces major and trace element, as well as $^{87}Rb/^{86}Sr$-$^{147}Sm/^{144}Nd$-$^{176}Lu/^{177}Hf$ compositions, of the two end-members in the martian mantle that mix in variable proportions to generate the range of compositions calculated for the shergottite sources (Borg and Draper, 2003).

The Borg and Draper (2003) model (hereafter 'BD03') was designed to explore the ability of a simple petrologic model for crystallization of a martian magma ocean to account for a range of geochemical observations from the martian meteorites. It uses experimentally determined phase relations to set the crystallization sequence, and then calculates the major and trace element composition of each crystallization 'package' based on element partitioning between the crystallizing solid and the residual liquid. The BD03 model successfully reproduces some important major and trace element characteristics of the martian source reservoirs such as the Ca/Al, Rb/Sr, Sm/Nd and Lu/Hf ratios. However, there are other characteristics, such as the relative LREE concentrations, that the model fails to reproduce. Accepting the inherent strengths and weaknesses of this model, which are discussed in detail by Borg and Draper (2003), we use this model to investigate the ability of a magma ocean scenario to explain the observed range in μ values in the sources of martian basalts. The goal is simply to determine if anhydrous silicates such as olivine, orthopyroxene and clinopyroxene and the oxide ilmenite can reproduce the U-Pb isotopic systematics of the shergottites, or whether additional phases or conditions are required.

In the BD03 model, the incompatible element-depleted end-member is the mafic cumulate pile formed from 5-90% crystallization of the martian magma ocean ('PCS (percent crystallized solid) steps' 2-4 from BD03; phases crystallize in constant proportions during each PCS step, but crystallization mode varies between PCS steps), and the incompatible element-enriched end-member is the trapped residual liquid remaining after 99.8% crystallization of the martian magma ocean. In this model,

crystallization of silicate phases alone controls the composition of source end-members. To account for the variations in source μ values between meteorites like QUE and meteorites like Zagami, crystallization of mantle phases such as garnet, olivine, orthopyroxene and clinopyroxene must fractionate U from Pb.

In the attempt to model the μ values of the martian mantle end-members with the BD03 model, we used the same parameters as used in the original model. The bulk composition of silicate Mars is from Lodders and Fegley (1997), and we adjusted the Pb concentration to 0.27 ppm so that bulk silicate Mars has a μ value of 3. This is consistent with observations from the shergottites that empirically constrain the μ value of the shergottite source region to ~3. The partition coefficients used in the model are listed in the caption of Figure 5. Although silicate crystallization alone generates cumulate packages with μ values that range from 0.7 to 3.9, the cumulate packages with the lowest μ values are also very depleted in incompatible elements (they are dominated by olivine and orthopyroxene), so they have very little leverage on the bulk composition of the combined cumulate package from PCS steps 2-4 (the 'mafic cumulate' depleted mantle end-member from BD03). Furthermore, these low-μ cumulate packages do not have the appropriate $^{87}Rb/^{86}Sr$, $^{147}Sm/^{144}Nd$ or $^{176}Lu/^{177}Hf$ ratios to serve as the source of the shergottites (Borg and Draper, 2003). The μ value calculated for the mafic cumulate end-member modeled as the source for QUE is 3.7. This is much higher than the μ value inferred for the depleted mantle end-member based on the U-Pb isotope data for QUE, and is even higher than the μ value of the modeled enriched end member (trapped residual liquid, $\mu = 3.2$). The low μ value (< 1.8) of the depleted QUE source is not

consistent with silicate-only crystallization in the magma ocean as illustrated in the BD03 model. Thus, the fundamental conclusion from this initial modeling effort is that the U/Pb composition of the martian mantle is unlikely to be controlled exclusively by crystallization of silicate phases.

The inability of the model to reproduce the μ values observed in the shergottites and its inability to account for substantial variation of μ in different sources suggests that crystallization of olivine ± orthopyroxene ± clinopyroxene ± ilmenite ± garnet does not alone control U-Pb fractionation in silicate Mars. It is possible that an additional process such as metasomatism plays a role in the formation of the martian source reservoirs. Alternatively, there may be a role for an additional phase in the petrogenesis of the mantle sources. Such a phase must strongly leverage the μ value but have a minimal effect on lithophile element ratios (Rb/Sr, Sm/Nd, Lu/Hf). Small amounts of sulfide co-precipitation with silicate phases during magma ocean crystallization is one possible mechanism to fractionate Pb from U and generate low-μ mafic cumulates without having any effect on the other elemental ratios of interest. It is a reasonable assumption that sulfide is involved in the formation of the QUE source region. Sulfides have been observed in QUE, indicating that the QUE parent magma inherited enough sulfur from its source to stabilize sulfide minerals (McKay et al., 1996). Shergottite Yamato 980459, which also is depleted in incompatible elements (McKay et al., 2004), likewise contains Fe-sulfide in its mesostasis (Mikouchi et al., 2004), further supporting the presence of sulfide in the depleted martian mantle source. Furthermore, as Mars is the 'volatile-rich planet' (e.g., Dreibus and Wänke, 1985), it is reasonable to infer that there should be

enough S in the planet to support a small amount of sulfide crystallization in the martian magma ocean, even assuming significant partitioning of S into the core (e.g., Wänke and Dreibus, 1994; Lodders and Fegley, 1997).

Crystallization of 0.36% sulfide during the PCS 4 step (0.36% relative to crystallization mode of PCS 4 step) incorporates a sufficient amount of Pb into this cumulate package to impart a low-μ (~1.9) composition on the 'mafic cumulate' end-member, represented by the combined 2-4 PCS steps. This small amount of sulfide crystallization results in a μ value for the depleted end-member consistent with that inferred from the μ value calculated for the QUE mantle source, but has minimal effect on the μ value of the enriched end-member (residual liquid). Crystallization of only a very small amount of sulfide is necessary to produce model results with μ values that are consistent with the observations from the martian meteorites. The amount of sulfide crystallization predicted by the models is inherently linked to both the partition coefficient for Pb in sulfide and the starting bulk composition for Mars. The partition coefficient that we used in these calculations, 2, is at the low end of the estimated range (Jones and Drake, 1986). Thus, 0.36% sulfide crystallization most likely represents a maximum estimate. In this model, sulfide saturation occurs in the middle-to-late stages (60-98%) of crystallization of the magma ocean. This implies that the martian magma ocean was not initially sulfur-saturated. However, progressive crystallization of silicates causes the S content of the remaining liquid to increase until the magma ocean becomes S-saturated, at which point sulfides begin to form and continue to form until the very latest stages of the magma ocean, when S is exhausted.

The results of these models illustrate the sizeable effect that very small amounts of sulfide crystallization can have on U/Pb ratios of geochemical reservoirs in a planet. Three-tenths of a percent sulfide crystallization, relative to the total magma ocean, results in enough redistribution of Pb to generate a two-fold variation in the μ values of geochemical reservoirs formed during magma ocean crystallization. In comparison, μ values in terrestrial reservoirs vary by a factor of ~1.2. This may indicate that phases such as sulfide, which generate such strong U-Pb fractionations, did not play a significant role in the formation of terrestrial geochemical reservoirs. Alternatively, large variation in μ values may have initially existed in Earth, but terrestrial reservoirs with distinctive μ values may have been effectively homogenized by mantle convection, melting and subduction, which has operated over ~3.5 billion years of Earth history. On the other end of the spectrum, μ values calculated for the lunar mantle display a range that varies by more than an order of magnitude (Premo et al., 1999). Thus, formation of the lunar mantle sources may involve either even greater extents of sulfide formation than we postulate for Mars or the operation of some additional process that can generate an additional order-of-magnitude in variation of the μ values.

5. CONCLUSIONS

Lead isotopic compositions of QUE mineral and whole rock fractions are extremely unradiogenic and show minimal variability. $^{206}Pb/^{204}Pb$ – $^{207}Pb/^{204}Pb$ – $^{208}Pb/^{204}Pb$ variation among all the QUE fractions indicates that this sample has suffered a minor amount of

terrestrial Pb contamination, presumably during its residence in Antarctic ice. Calculated amounts of contamination range from ~1 to ~7 % in the whole rock and purified silicate mineral separates, to ~ 80 % in the HCl leachates. Regardless of the small amounts of contamination in the purified mineral separates, these fractions define a line on a $^{238}U/^{204}Pb$ – $^{206}Pb/^{204}Pb$ plot that corresponds to an age of 397 ± 21 Ma and an initial $^{206}Pb/^{204}Pb$ of 11.086 ± 0.008. This age is only slightly older than the accepted crystallization age of 327 Ma, determined from the Rb-Sr and Sm-Nd systematics (Borg et al., 1997) and is therefore taken to be most representative of the QUE source. The initial Pb value determined for this sample corresponds to a μ value of 1.823 ± 0.008 for the source of QUE.

The μ value determined for the QUE source is the lowest value determined for any martian basalt. Based on comparison with Zagami, which has one of the highest estimated μ values for its source, we infer that the bulk μ value for Mars is ~ 3. With our new results for QUE, it is apparent that μ values in the martian source reservoirs vary by 100%. Furthermore, the μ values of the sources of martian basalts correlate broadly with Rb/Sr and Sm/Nd calculated for these same sources. Thus, the differentiation processes that control lithophile element ratios (Rb/Sr, Sm/Nd, Lu/Hf) in the martian sources also appear to control the U/Pb systematics. However, the U/Pb variation is not consistent with a magma ocean crystallization scenario in which silicates are the exclusive crystallizing phases. An additional phase or process is required to explain the observed variation in μ values. We successfully model the observed range in μ values with a small amount (0.3 %) of sulfide fractionation during the latest stages of magma ocean

crystallization. Modeling suggests that the presence of sulfide in magma ocean cumulates could account for the relatively large fractionation of U from Pb required by the meteorite data, while having minimal effect on the Rb/Sr, Sm/Nd and Lu/Hf ratios of the sources.

Acknowledgements – This work was supported by NASA Cosmochemistry grant NNG05GF83G to LEB and the Geology Foundation at The University of Texas at Austin. This work was performed under the auspices of the U. S. Department of Energy by the University of California, Lawrence Livermore National Laboratory under Contract No. W-7405-Eng-48.

REFERENCES

Beattie P. (1993) The generation of uranium series disequilibria by partial melting of spinel peridotite; constraints from partitioning studies. *Earth and Planetary Science Letters* **117**, 379-391.

Blichert-Toft J., Gleason J. D., Télouk P., and Albarède F. (1999) The Lu-Hf isotope geochemistry of shergottites and the evolution of the Martian mantle-crust system. *Earth and Planetary Science Letters* **173**, 25-39.

Borg L. E. and Draper D. S. (2003) A petrogenic model for the origin and compositional variation of the martian basaltic meteorites. *Meteoritics and Planetary Science* **38**, 1713-1731.

Borg L. E., Edmunson J. E., and Asmerom Y. (2005) Constraints on the U-Pb isotopic systematics of Mars inferred from a combined U-Pb, Rb-Sr, and Sm-Nd isotopic study of the Martian meteorite Zagami. *Geochimica et Cosmochimica Acta* **69**, 5819-5830.

Borg L. E., Nyquist L. E., Taylor L. A., Wiesmann H., and Shih C.-Y. (1997) Constraints on Martian differentiation processes from Rb-Sr and Sm-Nd isotopic analyses of the basaltic shergottite QUE 94201. *Geochimica et Cosmochimica Acta* **61**, 4915-4931.

Borg L. E., Nyquist L. E., Wiesmann H., and Reese Y. (2002) Constraints on the petrogenesis of Martian meteorites from the Rb-Sr and Sm-Nd isotopic systematics of the lherzolitic shergottites ALH77005 and LEW88516. *Geochimica et Cosmochimica Acta* **66**, 2037-2053.

Borg L. E., Nyquist L. E., Wiesmann H., Shih C.-Y., and Reese Y. (2003) The age of Dar al Gani 476 and the differentiation history of the martian meteorites inferred from their radiogenic isotopic systematics. *Geochimica et Cosmochimica Acta* **67**, 3519-3536.

Bouvier A., Blichert-Toft J., Vervoort J. D., and Albarède F. (2005) The age of SNC meteorites and the antiquity of the Martian surface. *Earth and Planetary Science Letters* **240**, 221-233.

Brandon A. D., Walker R. J., Morgan J. W., and Goles G. G. (2000) Re-Os isotopic evidence for early differentiation of the Martian mantle. *Geochimica et Cosmochimica Acta* **64**, 4083-4095.

Chen J. H. and Wasserburg G. J. (1986a) Formation ages and evolution of Shergotty and its parent planet from U-Th-Pb systematics. *Geochimica et Cosmochimica Acta* **50**, 955-968.

Chen J. H. and Wasserburg G. J. (1986b) S ≠ N =? C. *Lunar and Planetary Institute Conference Abstracts* **XVII**, 113-114.

Chen J. H. and Wasserburg G. J. (1993) LEW88516 and SNC meteorites. *Lunar and Planetary Institute Conference Abstracts* **XXIV**, 275-276.

Dreibus G. and Wänke H. (1985) Mars, a volatile-rich planet. *Meteoritics* **20**, 367-381.

Elliot T., Zindler A., and Bourdon B. (1999) Exploring the kappa conundrum: the role of recycling in the lead isotope evolution of the mantle. *Earth and Planetary Science Letters* **169**, 129-145.

Ewart A. and Griffin W. L. (1994) Application of proton-microprobe data to trace-element partitioning in volcanic rocks. *Chemical Geology* **117**, 251-284.

Foley C. N., Wadhwa M., Borg L. E., Janney P. E., Hines R., and Grove T. L. (2005) The early differentiation history of Mars from ^{182}W-^{142}Nd isotope systematics in the SNC meteorites. *Geochimica et Cosmochimica Acta* **69**, 4557-4571.

Harper C. L., Jr., Nyquist L. E., Bansal B., Wiesmann H., and Shih C. Y. (1995) Rapid Accretion and Early Differentiation of Mars Indicated by $^{142}Nd/^{144}Nd$ in SNC Meteorites. *Science* **267**, 213.

Harvey R. P., McCoy T. J., and Leshin L. A. (1996) Shergottite QUE 94201: texture, mineral compositions, and comparison with other basaltic shergottites. *Lunar and Planetary Institute Conference* **XXVII**, #497.

Hauri E. H., Wagner T. P., and Grove T. L. (1994) Experimental and natural partitioning of Th, U, Pb and other trace elements between garnet, clinopyroxene and basaltic melts. *Chemical Geology* **117**, 149-166.

Jones J. H. and Drake M. J. (1986) Geochemical constraints on core formation in the earth. *Nature* **322**, 221-228.

Kleine T., Mezger K., Munker C., Palme H., and Bischoff A. (2004) ^{182}Hf-^{182}W isotope systematics of chondrites, eucrites, and martian meteorites: Chronology of core formation and early mantle differentiation in Vesta and Mars. *Geochimica et Cosmochimica Acta* **68**, 2935-2946.

Lodders K. (1998) A survey of SNC meteorite whole-rock compositions. *Meteoritics & Planetary Science* **33**, 183-190.

Lodders K. and Fegley B. (1997) An Oxygen Isotope Model for the Composition of Mars. *Icarus* **126**, 373-394.

McKay G., Le L., Schwandt C., Mikouchi T., Koizumi E., and Jones J. (2004) Yamato 980459: the most primitive Shergottite? *Lunar and Planetary Science Conference* **XXXV**, 2154.

McKay G., Yang S. R., and Wagstaff J. (1996) Complex Zoned Pyroxenes in Shergottite QUE 94201: Evidence for a Two-Stage Crystallization History. *Lunar and Planetary Science Conference* **XXVII**, 851.

McKenzie D. and O'Nions R. K. (1991) Partial melt distributions from inversion of rare earth element concentrations. *Journal of Petrology* **32**, 1021-1091.

Mikouchi T., Koizumi E., McKay G., Monkawa A., Ueda Y., Chokai J., and Miyamoto M. (2004) Yamato 980459: Mineralogy and petrology of a new shergottite-related rock from Antarctica. *Antarctic Meteorite Research* **17**, 13.

Mikouchi T., Miyamoto M., and McKay G. A. (1996) Mineralogy and petrology of new Antarctic shergottite QUE94201: a coarse-grained basalt with unusual pyroxene zoning. *Lunar and Planetary Science Conference* **XXVII**, 879.

Misawa K., Nakamura N., Premo W. R., and Tatsumoto M. (1997) U-Th-Pb isotopic systematics of lherzolitic shergottite Yamato-793605. *Antarctic Meteorite Research* **10**, 95.

Misawa K., Yamada K., Nakamura N., Morikawa N., Kondorosi G., Yamashita K., and Premo W. R. (2006) Sm-Nd Isotopic Systematics of Lherzolitic Shergottite Yamato-793605. *Lunar and Planetary Science Conference* **XXXVII**, 1892.

Nyquist L. E., Bansal B. M., Wiesmann H., and Shih C.-Y. (1995) "Martians" young and old: Zagami and ALH 84001. *Lunar and Planetary Science Conference* **XXVI**, 1065.

Nyquist L. E., Reese Y., Wiesmann H., and Shih C.-Y. (2001) Age of EET79001B and implications for shergottite origins. *Lunar and Planetary Science Conference* **XXXII**, 1407.

Nyquist L. E., Reese Y. D., Wiesmann H., Shih C.-Y., and Schwandt C. (2000) Rubidium-strontium age of the Los Angeles shergottite. *Meteoritics & Planetary Science, Supplement* **35**, 121.

Nyquist L. E., Shih C. Y., Reese Y. D., and Irving A. J. (2004) Crystallization age of NWA 1460 shergottite: paradox revisited. *Second Conference on Early Mars: Geologic, Hydrologic, and Climatic Evolution and the Implications for Life*, 8041.

Nyquist L. E., Wooden J., Bansal B., Wiesmann H., McKay G., and Bogard D. D. (1979) Rb-Sr age of the Shergotty achondrite and implications for metamorphic resetting of isochron ages. *Geochimica et Cosmochimica Acta* **43**, 1057-1074.

Premo W. R., Tatsumoto M., Misawa K., Nakamura N., and Kita N. I. (1999) Pb-isotopic systematics of lunar highland rocks (>3.9 Ga); constraints on early lunar evolution. In *Planetary petrology and geochemistry; the Lawrence A. Taylor 60th birthday volume* (ed. G. A. Snyder, C. R. Neal, and W. G. Ernst), pp. 207-240. Bellwether Publishing.

Snyder G. A., Taylor L. A., and Neal C. R. (1992) A chemical model for generating the sources of mare basalts - Combined equilibrium and fractional crystallization of the lunar magmasphere. *Geochimica et Cosmochimica Acta* **56**, 3809-3823.

Stacey J. S. and Kramers J. D. (1975) Approximation of terrestrial lead isotope evolution by a two-stage model. *Earth and Planetary Science Letters* **26**, 207-221.

Symes S. J., Borg L. E., Shearer C. K., Asmerom Y., and Irving A. J. (2005) Geochronology of NWA 1195 based on Rb-Sr and Sm-Nd isotopic systematics. *Lunar and Planetary Science Conference* **XXXVI**, 1435.

Taylor S. R. (1980) Refractory and moderately volatile element abundances in the earth, moon and meteorites. *Lunar and Planetary Science Conference*, 333-348.

Vallelonga P., Gabrielli P., Rosman K. J. R., Barbante C., and Boutron C. F. (2005) A 220 kyr record of Pb isotopes at Dome C Antarctica from analyses of the EPICA ice core. *Geophysical Research Letters* **32**, 01706.

Wooden J., Shih C.-Y., Nyquist L., Bansal B., Wiesmann H., and McKay G. (1982) Rb-Sr and Sm-Nd isotopic constraints on the origin of EETA 79001: a second Antarctic shergottite. *Lunar and Planetary Institute Conference Abstracts*, 879-880.

Wänke H. and Dreibus G. (1994) Chemistry and accretion history of Mars. *Royal Society of London Philosophical Transactions Series A* **349**, 285-293.

Zartman R. E. and Richardson S. H. (2005) Evidence from kimberlitic zircon for a decreasing mantle Th/U since the Archean. *Chemical Geology* **220**, 263-283.

FIGURE CAPTIONS

Figure 1. Mineral separation scheme for QUE. Shaded boxes represent fractions analyzed.

Figure 2. (a) $^{206}Pb/^{204}Pb$-$^{207}Pb/^{204}Pb$ and (b) $^{206}Pb/^{204}Pb$-$^{208}Pb/^{204}Pb$ variation in whole rock, mineral and leachate fractions of QUE. In both panels, regression lines are drawn through all fractions, unless otherwise noted. Isotopic composition of modern terrestrial Pb is from Stacey and Kramers (1975) and Antarctic ice is from Vallelonga et al. (2005).

Figure 3. Symbols as in Figure 2. (a) ^{238}U-^{206}Pb diagram for QUE. Regression line drawn through WR (R), Plag (R) and MgPx (R) fractions (black symbols) gives the best age of 397 ± 21 Ma and initial $^{206}Pb/^{204}Pb$ of 11.086 ± 0.008. (b) ^{235}U-^{207}Pb diagram for QUE. No age information is preserved in this isotope system.

Figure 4. Calculated source compositions for the shergottites and Nakhla. All $^{87}Rb/^{86}Sr$, $^{147}Sm/^{144}Nd$ and $^{176}Lu/^{177}Hf$ points are from Borg and Draper (2003), which were calculated using data from Blichert-Toft et al. (1999), Borg et al. (1997; 2002), Nyquist et al. (1979; 1995; 2000; 2001) and Wooden et al. (1982), with the exception of Y79, which are from Borg et al. (2003) and Misawa et al. (2006). Calculations of μ values of shergottite and Nakhla sources are described in the text and use data from Chen and Wasserburg (1986a; 1986b; 1993), Misawa et al. (1997), Borg et al. (2005) and Bouvier

et al. (2005). Diamond symbols represent compositions of martian mantle end-member components; $^{87}Rb/^{86}Sr$, $^{147}Sm/^{144}Nd$ and $^{176}Lu/^{177}Hf$ values are the results of the BD03 model, and μ values are estimated empirically from isotopic variation of the shergottite sources.

Figure 5. Modeled μ values of martian magma ocean crystallization products. Diamond symbols represent μ values of cumulate packages calculated by the BD03 model with only silicate crystallization. Circle symbols represent results of the BD03 model, when 0.36% sulfide crystallization is included during the PCS 4 (60-90% crystallization) model step. In this model, the residual liquid remaining after 99.8% crystallization is the incompatible-element enriched mantle end-member dominantly sampled by Zagami, and the combined mafic cumulate package from PCS steps 2-4 is the incompatible element-depleted mantle end-member dominantly sampled by QUE.

Mineral-liquid partition coefficients for Pb used in the model are: 0.0005 for olivine, 0.0013 for orthopyroxene, 0.015 for clinopyroxene, 0.0001 for garnet, 0.5 for ilmenite and 2 for sulfide (from: Jones and Drake, 1986; McKenzie and O'Nions, 1991; Beattie, 1993; Ewart and Griffin, 1994; Hauri et al., 1994). Partition coefficients for U are: 0.0001 for olivine, 0.001 for orthopyroxene, 0.02 for clinopyroxene, 0.0001 for garnet, 0.00001 for ilmenite and 0.00001 for sulfide (from: Snyder et al., 1992; Borg and Draper, 2003).

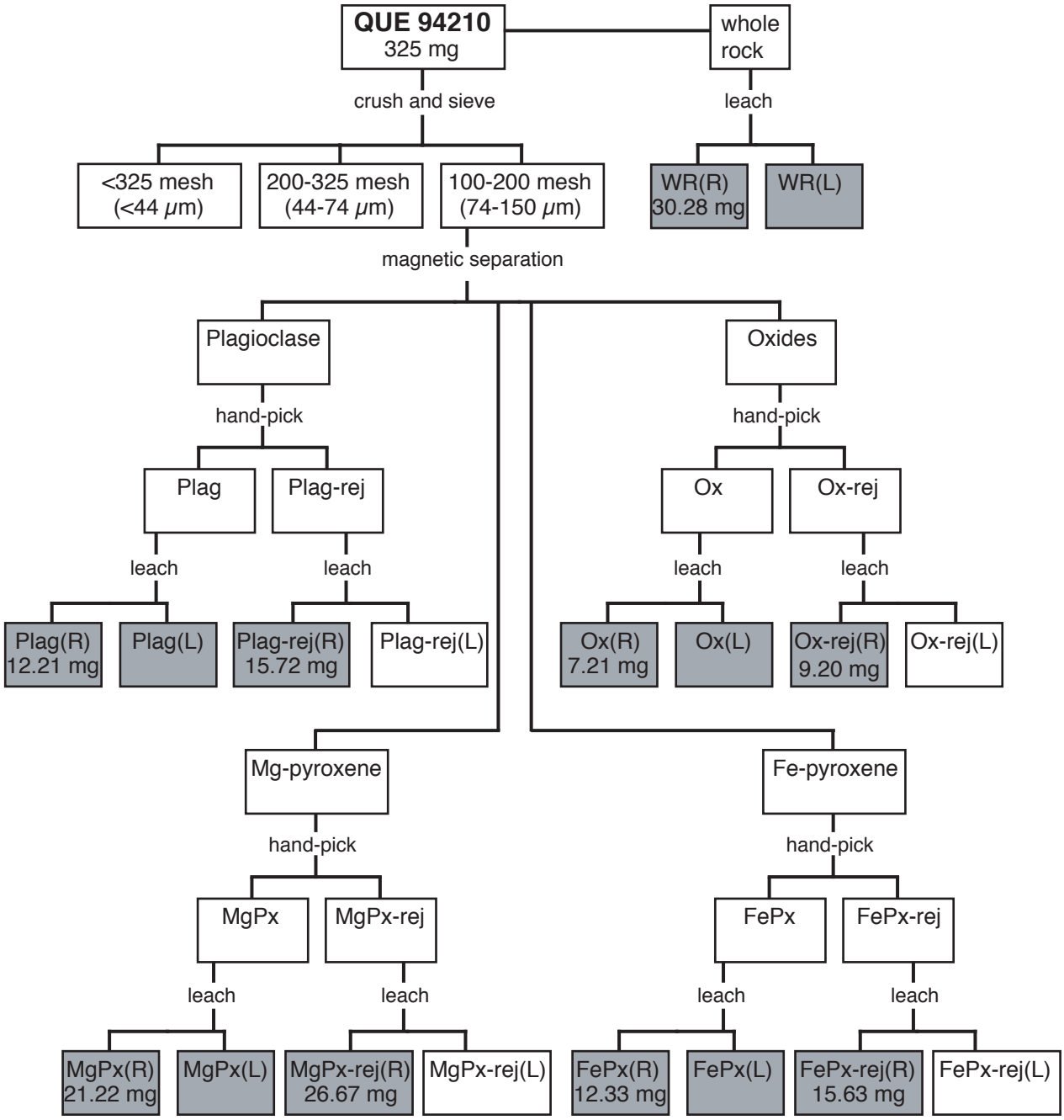

Figure 1
Gaffney et al.

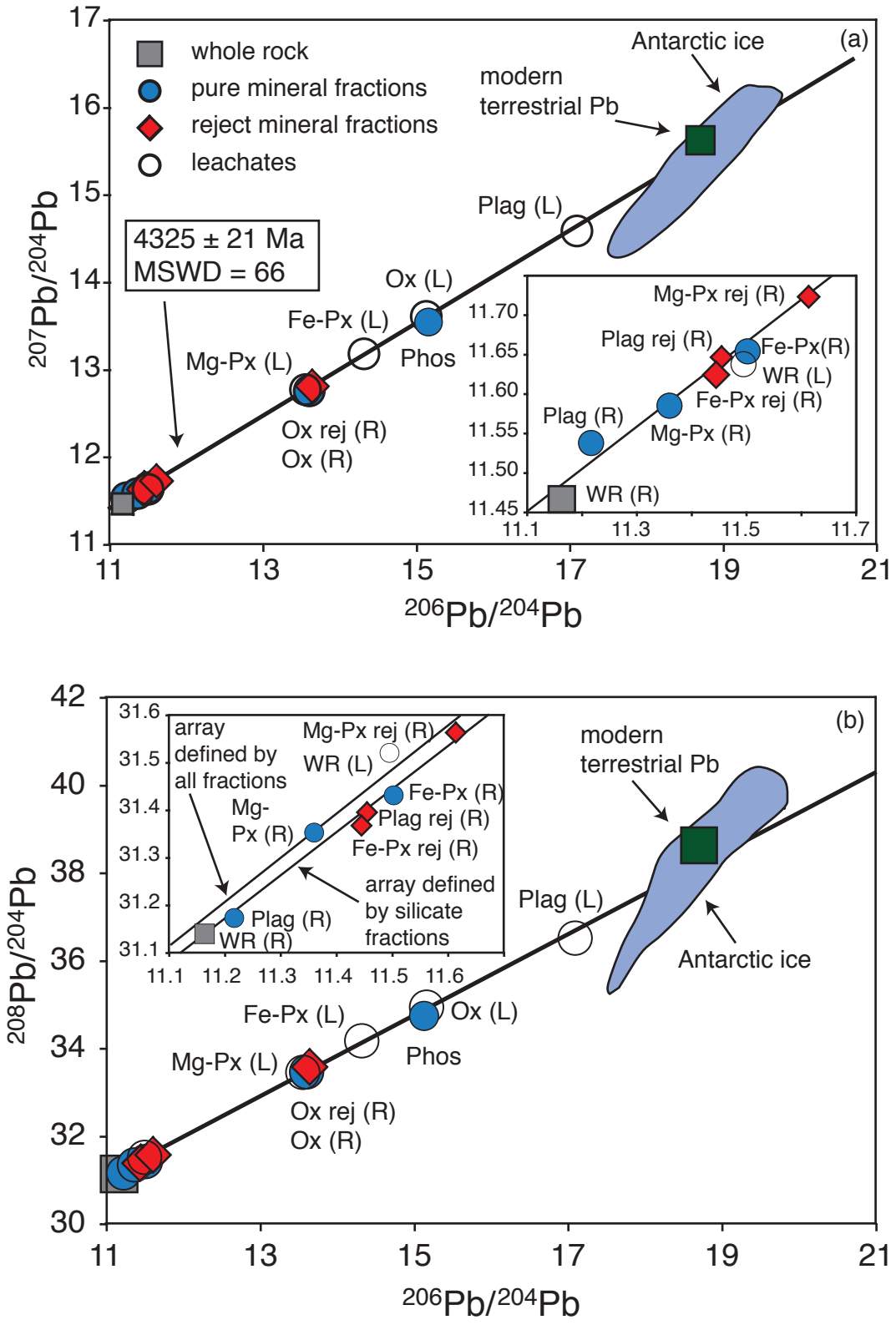

Figure 2
Gaffney et al.

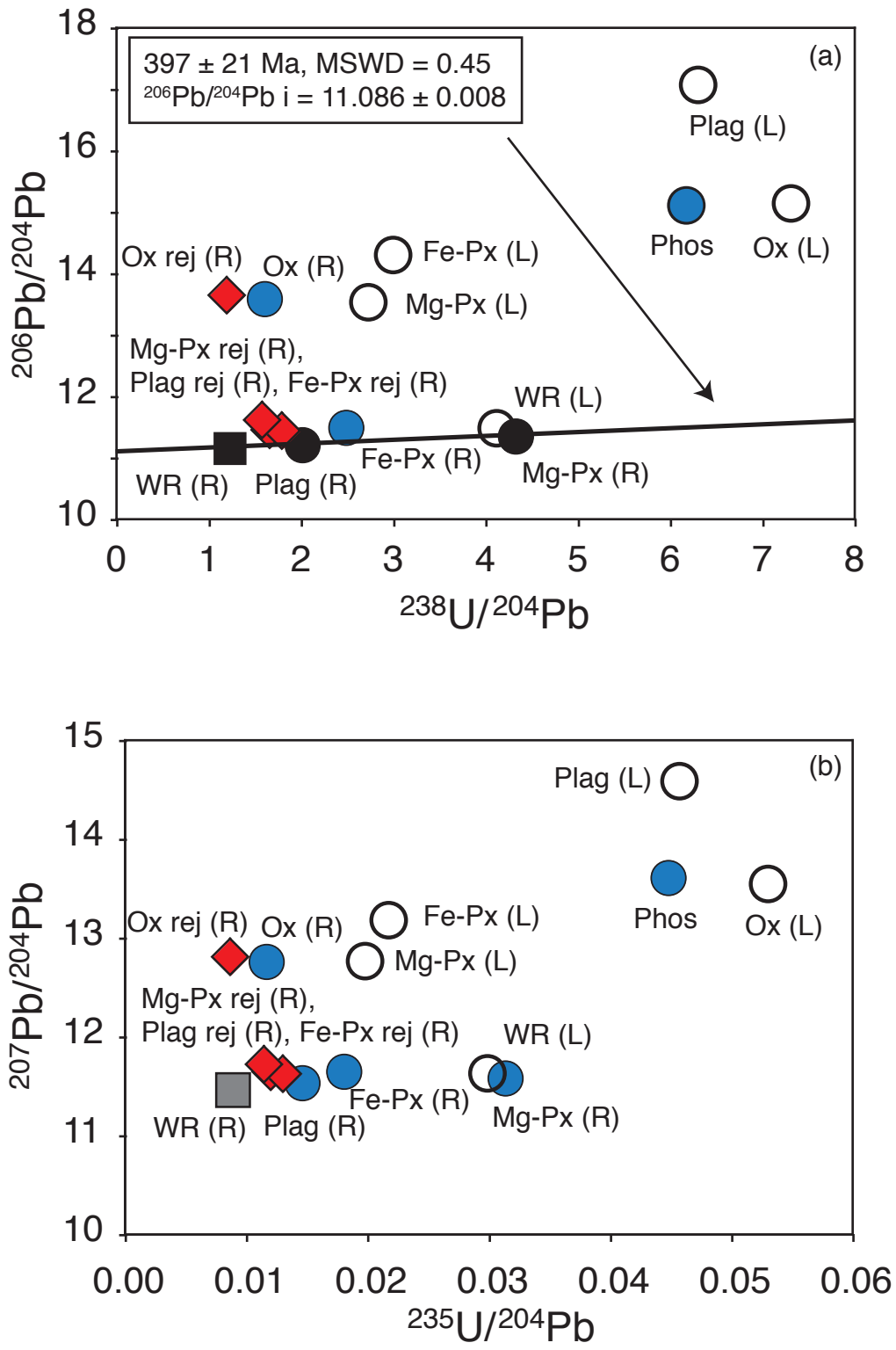

Figure 3
Gaffney et al.

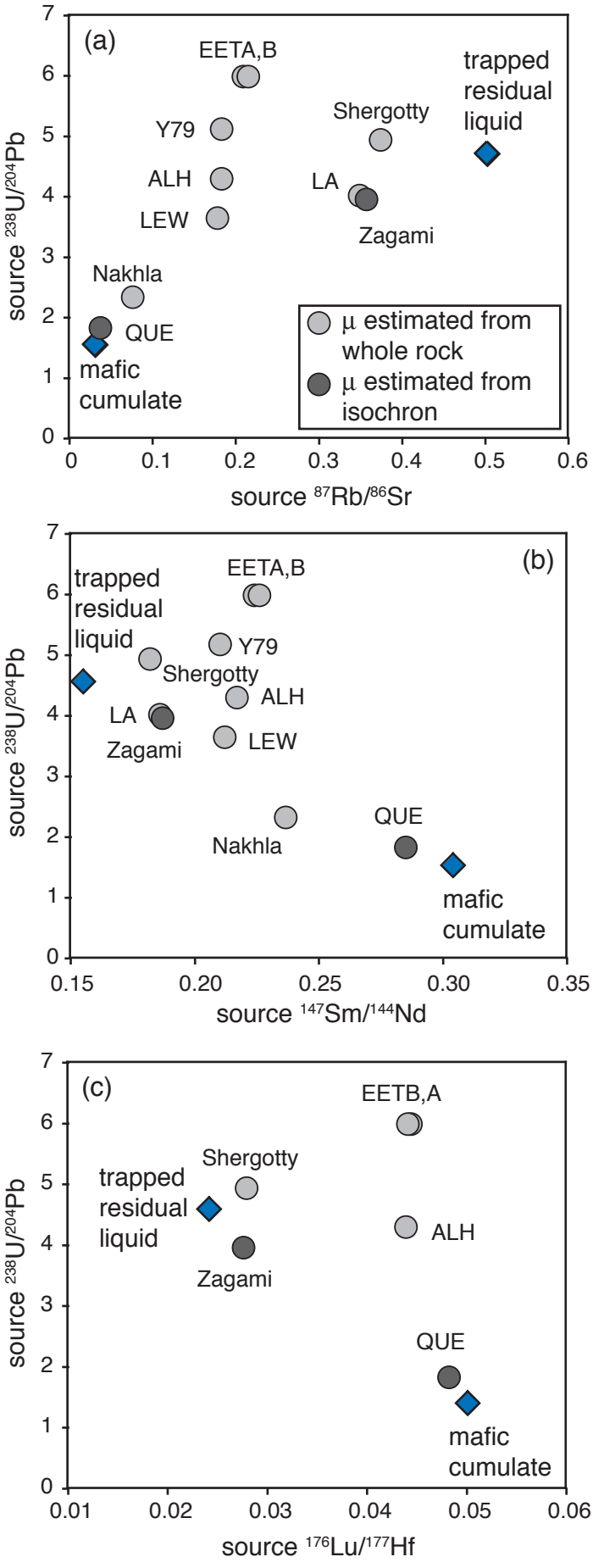

Figure 4
Gaffney et al.

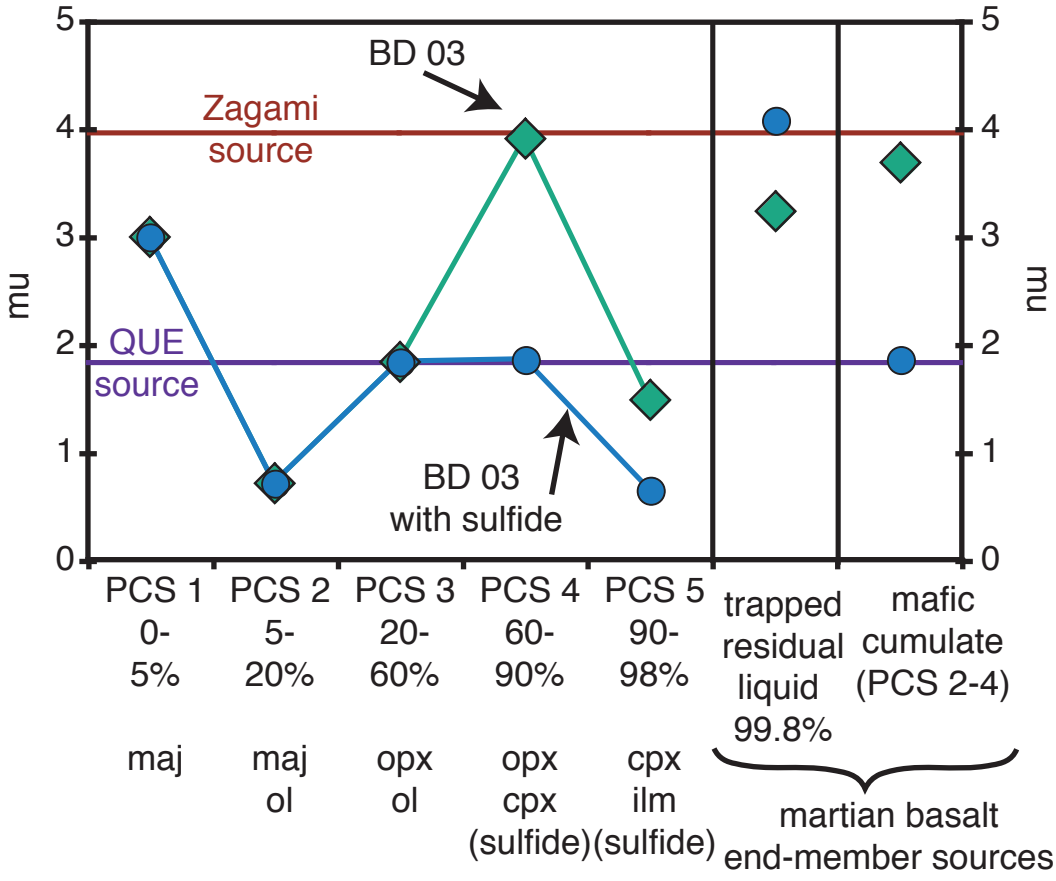

Figure 5
Gaffney et al.

Table 1: U-Pb isotopic compositions of QUE 94201

Fraction	wt. (mg)	U (ppm)	U (ng)	Pb (ppm)	Pb (ng)	$^{238}U/^{204}Pb^{a}$	±	$^{206}Pb/^{204}Pb^{b}$	±	$^{207}Pb/^{204}Pb^{b}$	±	$^{208}Pb/^{204}Pb^{b}$	±
Plag (R)	12.21	0.0023	0.028	0.054	0.660	2.0076	0.0081	11.2163	0.0088	11.5380	0.0090	31.174	0.028
Plag (L)			0.011		0.105	6.29	0.13	17.086	0.012	14.594	0.012	36.521	0.036
Plag rej (R)	15.72	0.0040	0.063	0.117	1.834	1.6569	0.0033	11.4550	0.0062	11.6463	0.0076	31.395	0.026
Mg-Px (R)	21.22	0.0014	0.030	0.016	0.336	4.320	0.058	11.359	0.010	11.5855	0.0096	31.353	0.028
Mg-Px (L)			0.037		0.715	2.7219	0.0091	13.5478	0.0079	12.7749	0.0087	33.466	0.028
Mg-Px rej (R)	26.67	0.0031	0.082	0.094	2.515	1.5775	0.0058	11.6141	0.0059	11.7228	0.0077	31.563	0.026
Fe-Px (R)	12.33	0.0016	0.020	0.031	0.379	2.481	0.018	11.502	0.015	11.654	0.013	31.432	0.036
Fe-Px (L)			0.022		0.399	2.987	0.029	14.312	0.018	13.186	0.015	34.180	0.041
Fe-Px rej (R)	15.63	0.0060	0.095	0.161	2.513	1.8032	0.0041	11.4450	0.0062	11.6240	0.0078	31.368	0.026
Ox (R)	3.23	0.0215	0.069	0.706	2.280	1.6002	0.0037	13.5983	0.0060	12.7647	0.0075	33.473	0.025
Ox (L)			0.090		0.692	7.302	0.017	15.153	0.011	13.554	0.011	34.950	0.032
Ox rej (R)	20.81	0.0089	0.185	0.392	8.150	1.1941	0.0012	13.6464	0.0052	12.8069	0.0071	33.564	0.025
Phos			0.002		0.022	6.17	0.41	15.121	0.046	13.614	0.039	34.752	0.093
Wr (R)	30.28	0.0029	0.089	0.114	3.454	1.2233	0.0019	11.1633	0.0047	11.4666	0.0066	31.140	0.023
Wr (L)			0.132		1.541	4.1130	0.0053	11.4946	0.0062	11.6380	0.0074	31.521	0.025

Plag = plagioclase, MgPx = Mg-rich pyroxene, FePx = Fe-rich pyroxene, Ox = oxide, Phos = phosphate, Wr = whole rock, (L) = HCl leachate, (R) = residue of HCl leachate, rej = portion of magnetically-separated mineral fraction rejected after hand-picking.

a. Error limits apply to last digits and include a minimum uncertainty of 0.5% plus 50% of the blank correction for U and Pb added quadratically.

b. Uncertainties refer to last digits and are $2\sigma_m$ calculated from the measured isotope ratios. $2\sigma_m = [\Sigma(m_i-\mu)^2/(n(n-1))]^{1/2}$ for n ratio measurements m_i with mean value μ.

c. Error limits refer to last digits and are $2\sigma_p$. $2\sigma_p = [\Sigma(M_i-\pi)^2/(N-1)]^{1/2}$ for N measurements M_i with mean value π.

Isochrons are calculated using either $2\sigma_p$ (from standard runs) or $2\sigma_m$ (from measured isotope ratios), whichever is larger.

Table 2: Estimates of terrestrial Pb contamination in fractions

Fraction	Pb total (ng)	calculated with Pb-Pb method				calculated with U-Pb method				(terr Pb by Pb-Pb method)/ (terr Pb by U-Pb method)
		sample Pb (ng)	terrestrial Pb (ng)	samp Pb/ terr Pb	% terr Pb in total sample	sample Pb (ng)	terrestrial Pb (ng)	samp Pb/ terr Pb	% terr Pb in total sample	
Plag (R)	0.660	0.644	0.015	41.617	2.35	0.657	0.003	242.609	0.41	5.72
Plag (L)	0.105	0.015	0.090	0.169	85.54	0.020	0.085	0.241	80.58	1.06
Plag rej (R)	1.834	1.713	0.121	14.206	6.58	1.741	0.093	18.653	5.09	1.29
Mg-Px (R)	0.336	0.320	0.016	19.433	4.89	0.333	0.003	100.579	0.98	4.97
Mg-Px (L)	0.715	0.429	0.287	1.497	40.06	0.446	0.270	1.654	37.69	1.06
Mg-Px rej (R)	2.515	2.281	0.235	9.704	9.34	2.315	0.201	11.541	7.97	1.17
Fe-Px (R)	0.379	0.351	0.028	12.500	7.41	0.359	0.020	18.309	5.18	1.43
Fe-Px (L)	0.399	0.196	0.203	0.964	50.92	0.206	0.193	1.069	48.33	1.05
Fe-Px rej (R)	2.513	2.352	0.161	14.613	6.41	2.394	0.119	20.187	4.72	1.36
Oxide (R)	2.280	1.349	0.931	1.448	40.85	1.383	0.898	1.540	39.37	1.04
Oxide (L)	0.692	0.261	0.430	0.607	62.22	0.303	0.389	0.780	56.19	1.11
Oxide rej	8.150	4.769	3.383	1.410	41.50	4.861	3.291	1.477	40.37	1.03
Phosphate	0.022	0.008	0.014	0.615	61.92	0.010	0.013	0.761	56.80	1.09
Wr (R)	3.454	3.406	0.048	70.649	1.40	3.443	0.011	303.920	0.33	4.26
Wr (L)	1.541	1.430	0.112	12.774	7.26	1.486	0.055	26.836	3.59	2.02